



NO_x storage and reduction in model lean NO_x trap catalysts studied by in situ DRIFTS

Yaying Ji ^a, Todd J. Toops ^b, Josh A. Pihl ^b, Mark Crocker ^{a,*}

^a Center for Applied Energy Research, University of Kentucky, 2540 Research Park Drive, Lexington, KY 40511, USA

^b Fuels, Engines and Emissions Research Center, Oak Ridge National Laboratory, 2360 Cherahala Boulevard, Knoxville, TN 37932, USA

ARTICLE INFO

Article history:

Received 26 January 2009

Received in revised form 28 May 2009

Accepted 1 June 2009

Available online 10 June 2009

Keywords:

DRIFTS

IR spectroscopy

Lean NO_x trap

NO_x adsorber catalyst

Ceria

ABSTRACT

NO_x storage and reduction on a model Pt/BaO/Al₂O₃ catalyst was studied by means of in situ DRIFTS measurements. To examine the effect of ceria addition, experiments were also conducted using Pt/BaO/Al₂O₃ to which Pt/CeO₂ was added as a physical mixture in a 74:26 weight ratio. For the former catalyst, DRIFT spectra acquired during NO/O₂ and NO₂/O₂ storage indicated the formation of nitrite at 200 °C during the initial stages of adsorption, while increasing the adsorption temperature appeared to facilitate the oxidation of nitrite to nitrate. The ceria-containing catalyst afforded similar DRIFT spectra under these conditions, although the presence of cerium nitrates was observed at 200 and 300 °C, consistent with NO_x storage on the ceria phase. DRIFT spectra acquired during NO_x reduction in CO and CO/H₂ showed that Ba nitrate species remained on the surface of both catalysts at 450 °C, whereas the use of H₂-only resulted in complete removal of stored NO_x. The observation of Ba carbonates when CO was present suggests that the inferior reduction efficiency of CO may arise from the formation of a crust of BaCO₃ on the Ba phase, which inhibits further NO_x reduction. DRIFT spectra acquired during lean-rich cycling (6.5 min lean, 1.0 min rich) with CO/H₂ as the rich phase reductants revealed that a significant concentration of nitrates remained on the catalysts at the end of the rich phase. This implies that a large fraction of nitrate is not decomposed during cycling and thus cannot participate in NO_x abatement through storage and regeneration.

© 2009 Published by Elsevier B.V.

1. Introduction

The effective removal of NO_x from the exhaust gas emitted by diesel and lean-burn gasoline engines represents an on-going challenge to the automotive industry. Lean NO_x trap (LNT) catalysts, also known as NO_x storage-reduction (NSR) catalysts, represent one of the more effective technologies for this purpose. The basis of the NO_x storage-reduction concept is a catalyst possessing dual functionality, comprising: (i) a storage function (in the form of a basic metal oxide, typically BaO) and (ii) a NO_x reduction component, typically composed of supported Pt and Rh metals. Under lean conditions NO is oxidized to NO₂ (over Pt) and stored on the metal oxide as a nitrate. Periodically a switch is made to reducing conditions, causing the NO_x to be released and converted to N₂ over the precious metal sites. The mechanism of NO_x storage and reduction on LNT catalysts has been extensively investigated and reviewed [1]. Most of these studies have focused on model catalysts of the type Pt/BaO/Al₂O₃; such catalysts are compositionally fairly simple, thereby facilitating mechanistic

studies, while nonetheless being reasonably representative of first generation LNT catalysts [2].

In the time since Toyota first disclosed the LNT concept, many combinations of precious metals, NO_x storage components, support materials, promoters and additives have been commercialized. Of these additional LNT catalyst components, we are particularly interested in ceria and the different functions it fulfills. Ceria is an important component of LNTs formulated for lean-burn gasoline applications, its role being to provide the necessary oxygen storage capacity when the engine is operating under stoichiometric conditions, i.e., when the LNT is required to function as a conventional three-way catalyst [3]. Recent studies have also shown that ceria possesses significant NO_x storage capacity [4–8], particularly at low to moderate temperatures (<400 °C), which may help to supplement the NO_x storage capacity of the main alkaline earth or alkali metal storage component. Ceria also promotes H₂ formation under rich conditions via the water–gas shift (WGS) reaction [9], which can be expected to facilitate catalyst regeneration and desulfation [10]. Additionally, ceria and ceria-zirconia can be beneficially employed as a support for the Ba phase in Ba-based LNTs [11–15]. Despite the many functions that ceria can be expected to fulfill, to date there have been relatively few studies specifically addressing the effect of ceria on LNT performance.

* Corresponding author. Tel.: +1 859 257 0295; fax: +1 859 257 0302.

E-mail addresses: crocker@caer.uky.edu (M. Crocker).

We have previously reported that the incorporation of ceria in Ba-based LNT catalysts significantly influences NO_x storage/reduction performance [16,17]. Studies using fully formulated catalysts showed that NO_x storage efficiency in the temperature range 150–350 °C increased with ceria loading, resulting in higher NO_x conversion levels. For model powder catalysts, the presence of ceria was found to improve NO_x storage capacity in the temperature range 200–400 °C under both continuous lean and lean-rich cycling conditions. Furthermore, temperature-programmed experiments showed that NO_x stored in a ceria-containing model catalyst was thermally less stable and more reactive to reduction with both H_2 and CO as compared to its ceria-free analog. In order to better understand the influence of ceria on NO_x storage and reduction, and in particular to obtain greater insight into the surface chemistry involved, we have applied *in situ* DRIFTS to the study of model powder LNT catalysts during both NO_x storage and reduction. Although a number of LNT catalyst studies employing FT-IR spectroscopy have been reported in the literature, they have mainly focused on Pt/Ba/Al₂O₃ type catalysts [18–30], although a few studies employing alkali metal based catalysts have also been reported [19,31–33]. In some cases this work has been extended to include investigations of catalyst sulfation and desulfation behavior [34–36]. Here, we report a DRIFTS study of model Ba-based LNT catalysts, both with and without added ceria. For the purposes of the study, catalysts were prepared consisting of Pt/BaO/Al₂O₃, as well as a physical mixture of Pt/BaO/Al₂O₃ and Pt/CeO₂. Ceria was incorporated as a physical mixture, rather than as a support for the BaO phase, since the latter option would have made it impossible to draw a fair comparison between the two catalysts; this follows from the fact that the BaO phases in the catalysts would be expected to possess different chemical and/or physical properties if present on different support materials.

2. Experimental

2.1. Catalyst preparation

The preparation of Pt/CeO₂ and Pt/BaO/Al₂O₃ powders has been described previously [16]. In brief, CeO₂ (Rhodia, surface area of 119 m²/g) was impregnated with an aqueous solution of tetraammineplatinum(II) nitrate. The impregnated sample was dried and then calcined in air at 500 °C for 3 h. Separately, γ -alumina (Sasol, surface area of 132 m²/g) was impregnated with aqueous Ba(NO₃)₂, dried and calcined at 500 °C in air. The Ba-loaded Al₂O₃ was subsequently impregnated with aqueous tetraammineplatinum(II) nitrate and further calcined at 500 °C. The Pt loading of both materials was 1 wt%, and the BaO content in the Pt/BaO/Al₂O₃ sample was 20 wt%. To prepare a ceria-containing LNT catalyst, a portion of Pt/BaO/Al₂O₃ was physically mixed with Pt/CeO₂ in a 74:26 weight ratio.

2.2. DRIFTS measurements

DRIFTS measurements were performed in an integrated stainless-steel reaction cell, using a MIDAC model M2500 FT-IR spectrometer coupled with a Harrick Scientific barrel ellipsoidal mirror DRIFTS accessory. This specially-designed DRIFTS assembly utilizes a barrel-shaped mirror that encompasses the catalyst sample [32,37]. With the sample at one focal point of the ellipsoid and the detector at the opposite focal point, the system collects roughly 300° of reflected IR signal and thus provides high sensitivity and high signal to noise ratios. The system is typically operated at slightly below atmospheric pressure (around 500 Torr) to prevent stagnation in the cell and to maintain the seal between the removable hemispherical ZnSe dome and the cell body. Tytan general mass flow controllers were used to establish the inlet gas

concentrations, in conjunction with a sparger system submerged in a recirculating constant temperature bath that controlled the inlet concentration of H₂O.

To minimize the initial spectral features associated with carbonates and achieve a good background spectrum, the catalysts were first pretreated in H₂ at 450 °C for at least 1 h, followed by NO_x storage at 300 °C for an additional 1 h. After heating to 450 °C again in H₂, initial background spectra were recorded every 50 °C in a decreasing sequence from 450 to 100 °C. The conditions for NO_x storage in this initial pretreatment consisted of 300 ppm NO (or 300 ppm NO₂) and 8% O₂ in Ar at 300 °C, DRIFTS spectra being collected periodically during the adsorption. Having minimized the initial carbonate features, the samples were ready for either storage evaluation, temperature programmed storage/reduction (TPSR), or lean/rich cycling experiments.

For the TPSR study, NO_x storage was repeated at 300 °C (300 ppm NO/8% O₂ for 1 h), followed by a brief purge in Ar and cooling to 100 °C. The sample was then exposed to reducing feed gas and heated in increments; the sample was maintained at each temperature step for 5 min. Spectra were recorded at 50 °C increments up to 450 °C by averaging 100 scans (scan rate = 2 scans/s). The reducing conditions consisted of one of the following: (i) 0.1% H₂, (ii) 0.3% CO, (iii) 0.1% H₂ + 0.3% CO or (iv) 0.3% CO + 5.0% H₂O. Although the temperature maximum in these experiments was dictated by the material constraints of the DRIFTS cell, the temperatures investigated correlate fairly well with those commonly encountered in diesel exhaust gas (~150–500 °C). This temperature range is somewhat lower than that typically encountered in lean-burn gasoline applications (~300–600 °C).

For the lean-rich cycling study, the sample was repeatedly exposed to lean and rich phases until eventually a “steady-state” cyclic condition was reached. This state is achieved when the final spectrum recorded at the end of the lean-phase is identical to the final lean spectrum of the preceding cycle; additionally, the corresponding final rich-phase spectra should also match for each cycle. A new spectrum was recorded every 10 s using an average of 10–15 scans (scan rate = 2 scans/s). The gas concentrations and times for each phase were: lean – 300 ppm NO, 8% O₂, 5% H₂O, 5% CO₂ in Ar for 6.5 min and rich – 5600 ppm CO, 3400 ppm H₂, 5% H₂O and 5% CO₂ in Ar for 1 min. These feed concentrations are reasonably representative of actual exhaust gas, with the exception that hydrocarbons were not included in the feed. However, many previous studies have shown that hydrocarbons are poor reductants in comparison with H₂ and CO [19,23,38,39], and so they are frequently omitted from simulated exhaust gas feeds (in this case it was a necessity to avoid interferences in the IR spectral region of interest).

It should be noted that in both the TPSR and lean-rich cycling experiments, N₂ and NH₃ were formed as the principle NO_x reduction products. Quantification of the selectivity to NH₃ was not possible due to the low gas flows employed and the interference of water with the NH₃ signal observed by mass spectrometry; however, we have previously reported selectivity data for catalysts PBA and PBAC during related NO_x reduction experiments [16].

3. Results and discussion

3.1. NO_x storage

3.1.1. Pt/BaO/Al₂O₃

NO_x storage on Pt/BaO/Al₂O₃, hereafter denoted as catalyst PBA, was first examined under flowing NO/O₂. As shown in Fig. 1a, for the first 20 s of exposure to NO/O₂ at 200 °C, the DRIFTS spectrum featured bands at 1556 and 1362 cm⁻¹, which can be ascribed to barium carbonate. Even though all of the bottled gases used in this study were of ultra high purity, and a CO₂ trap was used on the Ar

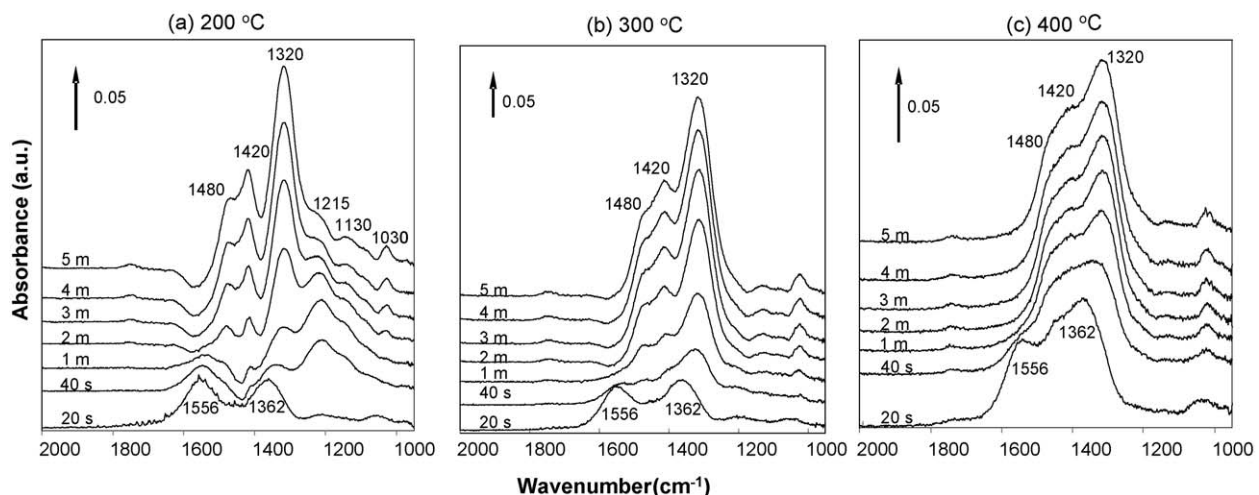


Fig. 1. DRIFT spectra recorded during exposure of PBA to NO/O_2 .

bottle, trace amounts of CO_2 were evidently present in the reactor which resulted in this absorbance. With increased exposure time, a new band appeared at ca. 1220 cm^{-1} , corresponding to Ba nitrite. This band reached a maximum after 1 min of exposure, after which it became weaker and two new bands grew in at 1420 and 1320 cm^{-1} , both of which can be assigned to Ba nitrate [28,29,35,40,41]. These bands became progressively more intense, such that after 5 min of exposure they dominated the spectrum. In addition, somewhat weaker bands were observed to grow in at 1480 and 1130 cm^{-1} which are assigned to another type of Ba nitrate. For the sake of bookkeeping and reference we have listed the observed absorption bands, along with their assignments, in Table 1. Compared to NO_x storage at $200\text{ }^\circ\text{C}$, spectra recorded at 300 and $400\text{ }^\circ\text{C}$ (Fig. 1b and c) failed to show any evidence of Ba nitrite formation prior to the appearance of Ba nitrate. The absence of Ba nitrite species at high temperature can be due to two reasons: either the fast kinetics of the direct oxidation of NO to NO_2 on Pt prior to adsorption on Ba, or the fast oxidation of initially formed Ba nitrite to give nitrate.

In the above discussion, the IR absorbances are only described in generic terms, i.e. barium nitrate rather than monodentate, bidentate or ionic nitrate. This is because the exact assignment of these three different types of nitrate is controversial. A recent

study by the Libuda group has helped to explain this controversy, as they have shown through predictive techniques that it is impossible to distinguish between monodentate and bridging Ba nitrate [42]. Another recent study by Roedel et al. has shown that the techniques used—transmission IR spectroscopy (TIRS), DRIFTS, attenuated total reflection infrared spectroscopy (ATR-IRS), polarization-modulation infrared reflection-absorption spectroscopy (PM-IRRAS)—lead to significantly different sensitivities, particularly with respect to bulk versus surface absorption bands [43]. In the latter study, the authors referenced many of the relevant earlier studies and the corresponding absorption bands which illustrate the discrepancies in the literature. For the purposes of this study, the simple generic description of barium or cerium nitrate is more than adequate to describe the processes occurring on these samples, so we will not attempt to define them in any more specific terms.

Compared to a number of studies reported in the literature concerning NO_x adsorption on model Ba-based LNT catalysts [22,28,30,43], the spectra reported here contain significantly fewer absorption bands. This difference results from the various treatment methods used prior to NO_x adsorption and the lower temperatures used for NO_x adsorption in most of these earlier studies. Whereas at high temperatures only NO_x species which interact strongly with the catalyst surface are present, corresponding to Ba-NO_x adsorbates, at room temperature the presence of NO_x adsorbed on Pt and alumina is also observed.

Fig. 2 shows the results of a storage experiment performed using a feed of flowing NO_2/O_2 . In contrast to the results obtained with NO/O_2 , Ba nitrite species (1215 cm^{-1}) were observed at an early stage of exposure at both 200 and $300\text{ }^\circ\text{C}$. However, the lifetime of the nitrite species formed at $300\text{ }^\circ\text{C}$ was considerably shorter than that observed at $200\text{ }^\circ\text{C}$ (~ 1 versus >5 min). After 40 s of adsorption at $300\text{ }^\circ\text{C}$, Ba nitrate became the main species present according to the spectra, the intensity of the nitrate bands increasing with time. Comparing the results from NO/O_2 and NO_2/O_2 adsorption, in both cases the formation of Ba nitrite was observed during the initial stages of adsorption, while increasing the adsorption temperature appeared to facilitate the transformation of nitrite to nitrate in both experiments. Several recent studies [18,28,40] have similarly concluded that NO_x storage can occur via NO adsorption to form nitrite, which subsequently undergoes oxidation to nitrate. A second mechanism for NO_x storage involves NO oxidation to NO_2 , followed by adsorption of NO_2 to form nitrate directly:



Table 1
Assignment of IR absorbances in DRIFT spectra.

Phase	Functional group	Wavenumber (cm^{-1})
Barium	Nitrate A ($-\text{NO}_3$)	1410–1423
		1314–1335
		1022–1037
	Nitrate B ($-\text{NO}_3$)	~1480
		~1130
	Nitrite ($-\text{NO}_2$)	1210–1220
Ceria	Carbonate ($-\text{CO}_3$)	1550–1560
		1345–1360
	Isocyanate ($-\text{NCO}$)	~2160
Alumina	Nitrate ($-\text{NO}_3$)	1540–1565
	Nitrite ($-\text{NO}_2$)	~1460
Platinum	Nitrate ($-\text{NO}_3$)	~1560
		1320–1323
	Isocyanate ($-\text{NCO}$)	2230
Gas	Carbonyl ($-\text{CO}$)	~2070
	CO_2	2360

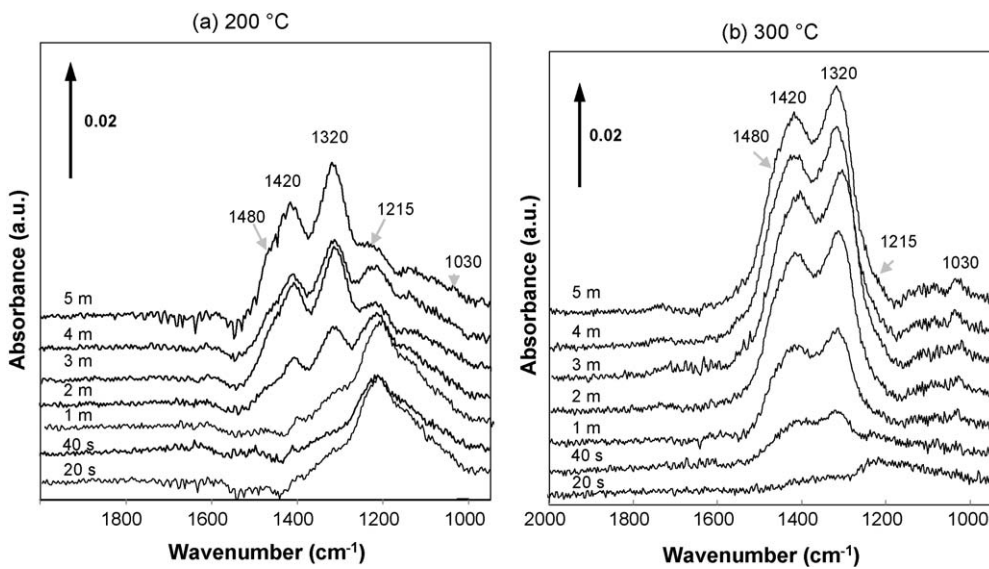


Fig. 2. DRIFT spectra recorded during exposure of PBA to NO_2/O_2 .

Eq. (1) represents a disproportionation reaction that has been discussed by several groups [18,27,30,44].

3.1.2. $\text{Pt}/\text{BaO}/\text{Al}_2\text{O}_3 + \text{Pt}/\text{CeO}_2$

To gain a better understanding of the positive impact of ceria addition on LNT NO_x storage properties, as reported in our previous study [16], NO_x adsorption on the physical mixture of $\text{Pt}/\text{BaO}/\text{Al}_2\text{O}_3$ and Pt/CeO_2 (hereafter denoted as PBAC), was investigated under flowing NO/O_2 and NO_2/O_2 . Spectra were again recorded at 200, 300 and 400 °C; given that the spectra acquired at 200 °C showed the greatest differences compared to those obtained for PBA, only the 200 °C spectra are shown (Fig. 3). From Fig. 3a, it is apparent that PBAC initially exhibited spectra similar to PBA upon exposure to NO/O_2 ; however, after 1 min of exposure, two new bands appeared at 1543 and 1523 cm^{-1} . These two bands are ascribed to two different vibrations of cerium nitrate [5]. With time, the intensity of these bands increased, along with that of the Ba nitrate bands. Different from NO/O_2 adsorption, only one extra band at

~1562 cm^{-1} appeared after 1 min of exposure to NO_2/O_2 (Fig. 3b), this band again being assigned to a nitrate species on ceria. These findings are consistent with our previous reports [16,17] that ceria is able to store NO_x , thereby supplementing the main Ba NO_x storage material and improving NO_x storage capacity, particularly at low temperatures. At higher temperature, the intensity of the cerium nitrate bands was diminished relative to the Ba nitrate bands, such that at 400 °C they were no longer visible. This accords with our previous finding that the benefits of ceria addition, in terms of NO_x storage-reduction performance, are negligible at 400 °C [16].

3.2. Reduction of stored NO_x

3.2.1. H_2 and CO as reductants

The reduction of NO_x stored on PBA was performed using both H_2 and CO as reductants. Prior to performing NO_x reduction, NO_x was first stored on the sample by exposure to flowing NO/O_2 at

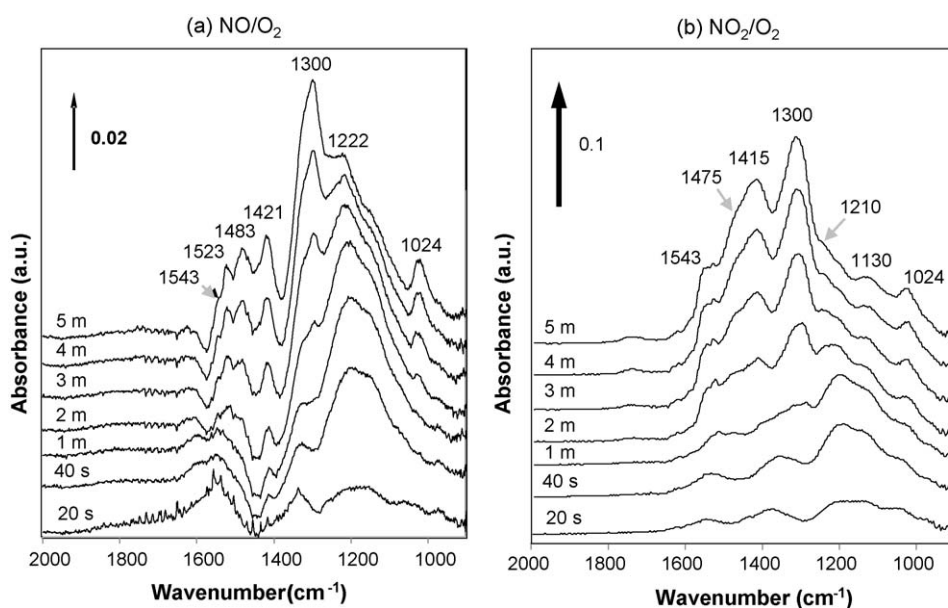


Fig. 3. DRIFT spectra recorded during exposure of PBAC to NO/O_2 and NO_2/O_2 at 200 °C.

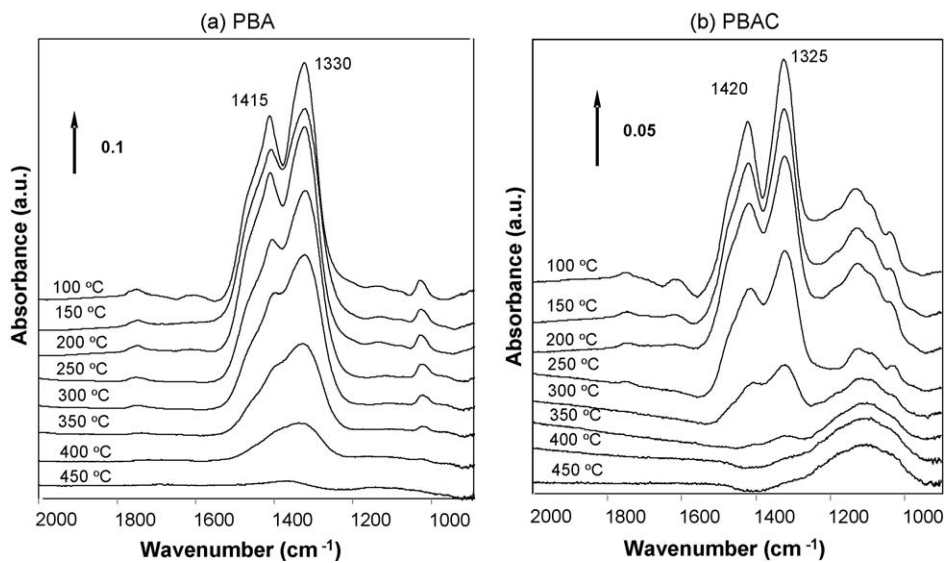


Fig. 4. DRIFT spectra recorded during H_2 -TPR over PBA and PBAC with NO_x stored at $300\text{ }^\circ\text{C}$.

$300\text{ }^\circ\text{C}$ for 1 h, after which the system was flushed with Ar, cooled to $100\text{ }^\circ\text{C}$ and then exposed to the reductant. Fig. 4a shows a series of spectra collected under H_2 at increasing temperature. The only IR absorption bands present in the spectra were those corresponding to Ba nitrate (1420 and 1320 cm^{-1}), the intensity of which was observed to diminish with increasing temperature. At $450\text{ }^\circ\text{C}$, the nitrate bands disappeared completely, indicating that all of the stored NO_x was removed. This temperature is much higher than that reported by Szailer et al. [22] for $\text{Pt}/\text{Ba}/\text{Al}_2\text{O}_3$, who reported complete nitrate removal under H_2 at $300\text{ }^\circ\text{C}$. This is most likely correlated to the use of different temperatures for NO_x storage; in their studies, NO_x was stored at ambient temperature rather than at $300\text{ }^\circ\text{C}$. At ambient temperature, there is a large amount of potential storage sites [33], but the adsorption of the nitrates into the bulk is slow and without a very long exposure they will not migrate into the bulk where the most stable adsorption occurs.

Corresponding spectra acquired for PBAC during H_2 -TPR are shown in Fig. 4b. Examining the spectra for PBAC and PBA in the temperature range 250 – $450\text{ }^\circ\text{C}$, and comparing the decrease in intensity of the nitrate bands at 1420 and 1330 cm^{-1} in each set of spectra (in each case relative to the initial intensity at $100\text{ }^\circ\text{C}$), it is apparent that nitrate species on PBAC are removed at a slightly

lower temperature. This result is consistent with our previously reported temperature-programmed microreactor experiments [16], in which NO_x stored on PBAC was found to be thermally less stable and more reactive to reduction with both H_2 and CO as compared to PBA. The improved regeneration characteristics of PBAC are likely a consequence of the competitive capture of NO_x by the Pt/CeO_2 component, which results in reduced formation of bulk $\text{Ba}(\text{NO}_3)_2$ in PBAC relative to PBA. Upon exposure to NO_x , surface nitrates are initially formed on BaO , while increased exposure results in the subsequent formation of bulk nitrates, corresponding either to nitrates stored at sites remote from Pt and/or crystalline Ba nitrate. Peden and co-workers [45] have shown that bulk $\text{Ba}(\text{NO}_3)_2$ is significantly more difficult to reduce than surface $\text{Ba}(\text{NO}_3)_2$.

Relative to reduction in H_2 , spectra obtained under CO were more complicated (Fig. 5a). Given that the spectra for PBA and PBAC were qualitatively similar, only the spectra obtained for PBA are considered here. Besides the Ba nitrate bands formed during the initial NO_x storage, new bands appeared which can be assigned to Ba carbonate (1550 cm^{-1}), Pt-CO (2067 cm^{-1}), Ba-NCO (2162 cm^{-1}) and gas-phase CO_2 (2329 and 2360 cm^{-1}) [18,22,23]. In addition, a very weak band corresponding to Al-

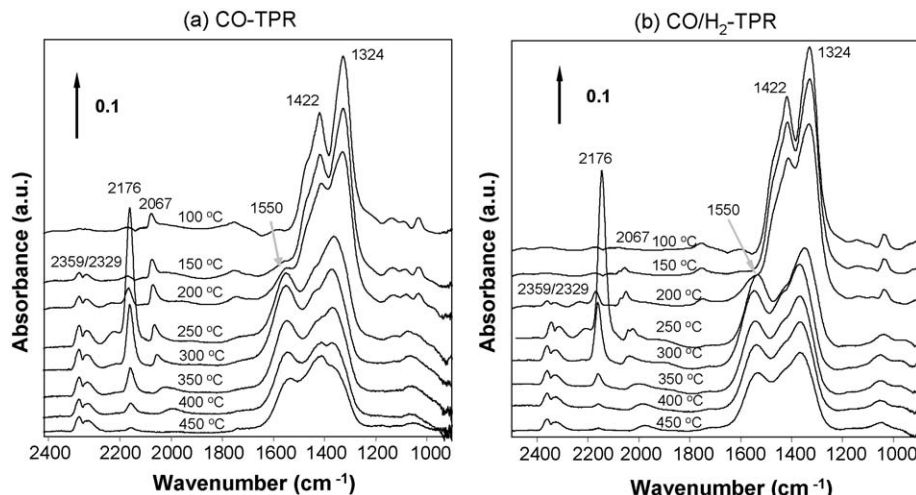


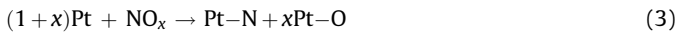
Fig. 5. DRIFT spectra recorded during CO- and CO/H_2 -TPR over PBA with NO_x stored at $300\text{ }^\circ\text{C}$.

bound NCO (2230 cm^{-1}) was observed at $250\text{ }^\circ\text{C}$ [22,23]. Between 200 and $250\text{ }^\circ\text{C}$ the intensity of the nitrate bands diminished noticeably, after which further increase in the temperature produced only a relatively small decrease in band intensity. At $450\text{ }^\circ\text{C}$, Ba nitrate species remained on the surface, an indication that CO, unlike H_2 , was not able to fully reduce the stored NO_x under these conditions. This observation is consistent with previous reports that CO is a less active NO_x reductant than H_2 [16,22,38,46,47]. The inferior reduction efficiency of CO in TPR may arise in part from the formation of a crust of Ba carbonate on the Ba phase (via the reaction of CO_2 and BaO), which inhibits further reduction of the stored NO_x . Consistent with this idea, at $200\text{ }^\circ\text{C}$ a band started to grow in at 1550 cm^{-1} characteristic of bidentate carbonate ($\nu_{\text{C=O}}$) [18]. Other bands in the region $\sim 1340\text{--}1410\text{ cm}^{-1}$, present in the spectra acquired in the temperature range $250\text{--}450\text{ }^\circ\text{C}$, may be assigned to the superposition of the residual 1422 and 1324 cm^{-1} Ba nitrate bands and the corresponding asymmetric stretching band of the carbonate ($\nu_{\text{OCO asym}}$, 1345 cm^{-1} [18]).

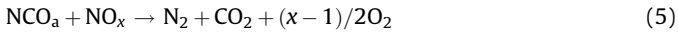
In the case of the Pt–CO band, this was clearly observable in the temperature range $100\text{--}300\text{ }^\circ\text{C}$. At $150\text{ }^\circ\text{C}$, the formation of gas phase CO_2 was observable, although no reduction in nitrate intensity was evident at this stage. Evidently, at this low temperature the Pt–CO bond is quite stable and therefore CO spillover onto the storage phase and subsequent nitrate release is not significant. However, the observation of CO_2 suggests that some CO was consumed at this low temperature by reaction with oxygen atoms adsorbed on Pt during the prior NO_x storage at $300\text{ }^\circ\text{C}$:



Upon raising the temperature to $200\text{ }^\circ\text{C}$, the formation of Ba–NCO was observed, the intensity of this band reaching a maximum at around $250\text{ }^\circ\text{C}$. This is coincident with the temperature at which nitrate removal became significant, as evidenced by the decrease in the intensity of the nitrate bands observed on raising the temperature from 200 to $250\text{ }^\circ\text{C}$. Further heating resulted in a pronounced decline in the intensity of the Ba–NCO band. These observations suggest a sequence of reactions involving (i) CO adsorption on Pt and spillover to the storage phase, (ii) nitrate decomposition and NO_x release, (iii) NO_x dissociation on the reduced Pt sites (Eq. (3)) and (iv) isocyanate formation (Eq. (4)):



Evidently, the isocyanate formed spills over onto the Ba phase (and to a much lesser extent, the alumina support). We note that this sequence is consistent with the reaction scheme proposed by Szailor et al. [22]. The same group also proposed that isocyanate decomposition proceeds via its reaction with NO_x , e.g.:



where NCO_a indicates that the species is adsorbed on the Ba-phase. For simplicity, and to differentiate between molecules adsorbed on Pt and those adsorbed on the Ba or alumina phase, the subscript “a” will be used for all non-Pt adsorptions. From the spectra in Fig. 5a it is apparent that the reduction in Ba–NCO band intensity at progressively higher temperatures was accompanied by a modest decrease in the intensity of the nitrate bands. This is consistent with the reaction depicted in Eq. (5), although we cannot rule out that other isocyanate decomposition pathways may be operative, such as the reverse of Eq. (4), with subsequent desorption of N_2 .

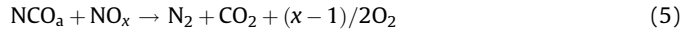
While the preceding sequence describes the chemistry that is apparent on the surface, it is not clear at which point N_2 is formed.

The observations suggest that there are two CO-routes that could be followed that enable the removal of NO_x and the formation of N_2 . Both routes require CO to first adsorb on Pt, then spillover onto the storage phase and cause the release of nitrates, as has been reported elsewhere [48]. This release of nitrates must be initiated by CO below $300\text{ }^\circ\text{C}$, since our microreactor and DRIFTS TPD results show that in the absence of a reductant there is not significant release of NO_x below the adsorption temperature of $300\text{ }^\circ\text{C}$. The first route is the simplest path; the released NO_x adsorbs on Pt, dissociates via Eq. (3), and then N_2 is formed via a simple adjacent site reaction as shown below:



Adsorbed oxygen is then removed by reaction with CO (Eq. (2)) to close the catalytic cycle. This route implies that the observed NCO is simply a spectator. However, while NCO may not directly contribute to the formation of N_2 , it would have a crucial role in freeing up Pt sites for the NO_x dissociation reaction in Eq. (3). At these low temperatures, where there is a significant Pt–CO feature, $\sim 2070\text{ cm}^{-1}$, it is important that CO is removed from the Pt sites and transferred to the Ba-phase either through the direct spillover route or after NCO is formed. Formation of Ba-based carbonate, 1555 and 1350 cm^{-1} , is observed at the same temperature that Ba-based NCO is observed, beginning at $200\text{ }^\circ\text{C}$; therefore, it is not possible to differentiate whether CO or NCO spillover is more important. Regardless, both mechanisms result in additional Pt sites for NO dissociation, and, since the Pt–CO concentration is being depleted, it also increases the probability of a Pt–N species reacting with another Pt–N and forming N_2 , thus completing the catalytic cycle.

The second route to consider suggests NCO has a more active role in the mechanism. As before, CO spillover initiates NO_x release, NO dissociates on the Pt as in Eq. (3), and NCO forms as in Eq. (4). However, instead of simply spilling over onto the Ba-phase, it also actively reacts with NO_x as Szailor et al. [22] have suggested:



This is not an elementary reaction, and several different reaction pathways could be used to describe this step. In principle, Eq. (5) could correspond to a direct Ba-based reaction of NCO with a surface nitrate, $(\text{NO}_3)_a$, leading to a surface carbonate, or a Pt-based reaction that occurs after the NCO readsorbs onto the Pt phase, or even NCO reacting directly with gas-phase NO_x (invoking an Eley–Rideal mechanism). All of these routes invoke a more complex reaction mechanism than the one previously described, and until more rigid experimental evidence supporting one of these routes is available, further discussion is not merited.

Considering that H_2 and CO co-exists in the exhaust gas stream under practical operating conditions, an experiment employing a mixture of H_2/CO (1000 ppm H_2 and 3000 ppm CO) as reductant was carried out. As with the use of CO as reductant, a marked decrease in the intensity of the nitrate bands was observed at around $200\text{ }^\circ\text{C}$ (Fig. 5b), after which only a slight decrease in band intensity was observed with increasing temperature. However, compared to the spectra obtained using CO-only, the Pt–CO band did not appear until $150\text{ }^\circ\text{C}$ (versus $100\text{ }^\circ\text{C}$ for the CO-only case), and the intensity of the band was weaker at all temperatures. Furthermore, gas phase CO_2 was not formed until a temperature of $200\text{ }^\circ\text{C}$ was attained (versus $150\text{ }^\circ\text{C}$ for the CO-only case). These observations suggest that at low temperatures the Pt surface is mainly covered by H_2 , which is responsible for the reduction of the Pt particles. It is also interesting to note that the Ba–NCO band was

more intense at its maximum for the spectrum collected under H_2 versus CO , as measured relative to the intensity of the nitrate bands in the respective spectra. This is consistent with previous studies in which the presence of H_2 was found to promote isocyanate formation from NO and CO over a variety of metals dispersed on oxidic supports [49,50]. This effect has been attributed to the promotion of NO dissociation when H_2 is present, most likely due to enhanced electron donation from the metal to the NO antibonding orbital when adsorbed hydrogen is present on the metal surface [51]. At temperatures of 300 °C and higher there was very little difference between the spectra obtained under CO and CO/H_2 . In both cases bands were observed corresponding to residual nitrate, implying that the extent of NO_x reduction was similar. The fact that the presence of H_2 did not result in a significant enhancement of NO_x reduction can be attributed to the formation of Ba carbonate, the presence of which was again evidenced by the $\nu_{\text{C=O}}$ band at 1550 cm^{-1} . Evidently, this type of carbonate is stable to the presence of H_2 under these conditions.

3.2.2. Effect of H_2O

CO-TPR of stored NO_x was also studied in the presence of H_2O . In the case of catalyst PBA, the $\text{Ba}-\text{NCO}$ band was much weaker than for the corresponding spectra acquired in the absence of water, and completely disappeared at around 300 °C (Fig. 6a). This can be ascribed to hydrolysis of the $\text{Ba}-\text{NCO}$ groups to afford NH_3 and CO_2 [22,46]. In the presence of water, the two Ba nitrate bands at 1420 and 1320 cm^{-1} tended to become one broad band located at around 1400 cm^{-1} . Westerberg and Fridell [52] assigned this band to “bulk” nitrate, while Szailer et al. [22] demonstrated that as a consequence of its increased mobility, surface nitrate can transform to “bulk” nitrate in the presence of water vapor. In principle, this type of nitrate can correspond to either nitrate crystallites or to nitrate located far away from the Pt sites. With increasing temperature, the Ba nitrate band became narrower and weaker, although residual nitrate appeared to be present at 450 °C. In general, the addition of H_2O appeared to inhibit the formation of Ba carbonate, as evidenced by the weaker Ba carbonate band at 1550 cm^{-1} observed with H_2O present relative to reduction performed with CO -only.

Compared to PBA, spectra acquired for PBAC showed two main differences (Fig. 6b). Firstly, unlike PBA, the isocyanate band at 2170 cm^{-1} was not observed. Secondly, the $\text{Pt}-\text{CO}$ band at 2050 cm^{-1} disappeared at a lower temperature than for PBA

(~250 versus ~300 °C). Both of these observations are indicative of increased CO reactivity on PBAC, as compared to PBA. In principle there are three main pathways for CO consumption, comprising reaction with stored NO_x , participation in the water-gas shift (WGS) reaction, and oxidation by reaction with stored oxygen. Given the presence of ceria in PBAC, the latter pathway can be expected to be more significant for PBAC than PBA, although this does not represent a route for continuous CO removal once the ceria is reduced.

In order to clarify the role of H_2O in the reduction of stored NO_x with CO , the reaction of CO with H_2O was examined over clean samples of PBA and PBAC (i.e., without stored NO_x). Previous microreactor experiments have indicated that PBAC is a more active water-gas shift catalyst than PBA [16], an observation which can be ascribed to the presence of Pt/CeO_2 in PBAC. As shown in Fig. 7, DRIFTS results confirm this finding. For PBA, the water-gas shift reaction commenced at around 150 °C, as evidenced by the observation of very weak gas-phase CO_2 bands (Fig. 7). At 100 °C a $\text{Pt}-\text{CO}$ band was visible at around 2060 cm^{-1} , which disappeared upon raising the temperature to 300 °C. In the case of PBAC, weak bands corresponding to CO_2 were already visible at 100 °C, together with a strong $\text{Pt}-\text{CO}$ band. At 150 °C significant CO_2 production was observed, consistent with the almost complete disappearance of the $\text{Pt}-\text{CO}$ absorption band. These findings clearly demonstrate that PBAC is more active at low temperatures for the WGS reaction than PBA. Although the generation of H_2 via the WGS reaction should result in more facile nitrate reduction than when using CO only as the reductant, the presence of strong carbonate bands partially obscured the nitrate region of the spectra, rendering it impossible to quantify whether reduction in $\text{CO}/\text{H}_2\text{O}$ indeed proceeds more efficiently than in CO only. However, we note that a number of previous reactor studies have shown this to be the case [53], including our own microreactor study using PBA and PBAC [16].

3.3. Lean-rich cycling

In order to gain insight into the storage-reduction properties of the model catalysts under working conditions, DRIFT spectra were recorded during lean-rich cycling (6.5 min lean and 1.0 min rich). To simulate realistic exhaust gas, H_2O and CO_2 were included in the feed gas in both the lean and rich phases, and a mixture of CO and H_2 was used as the rich phase reductant. Shown in Fig. 8a are

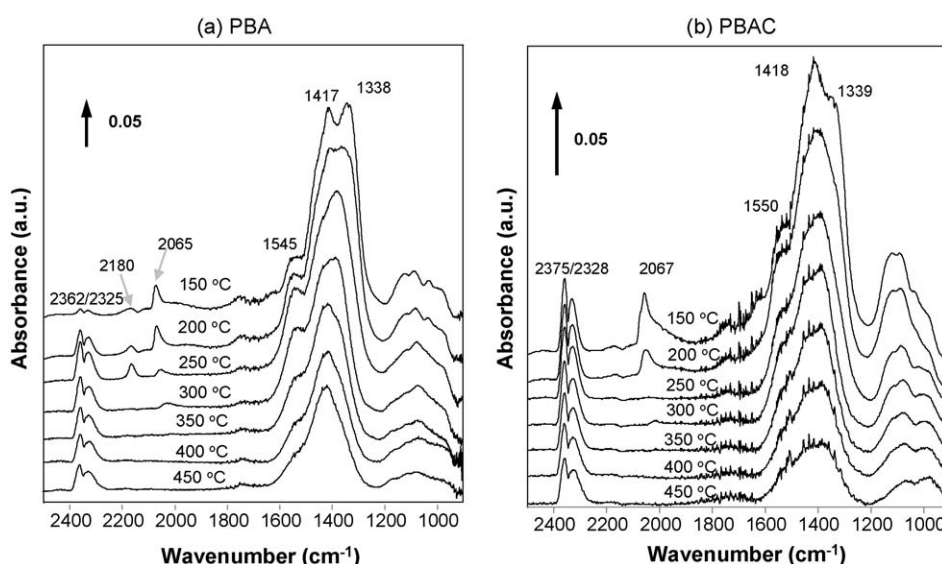


Fig. 6. DRIFT spectra recorded during $\text{CO}/\text{H}_2\text{O}$ -TPR over PBA and PBAC with NO_x stored at 300 °C.

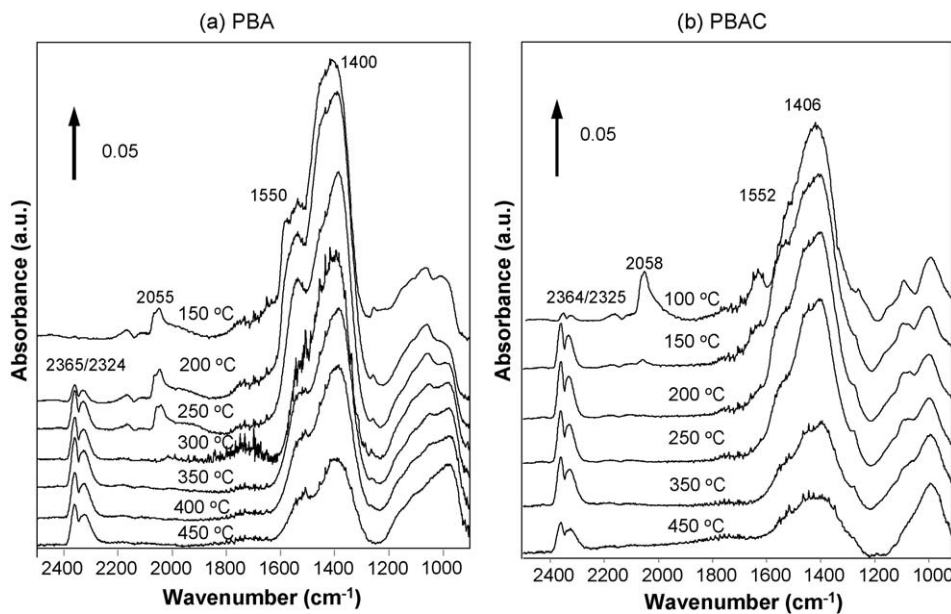


Fig. 7. DRIFT spectra recorded during water-gas shift reaction over PBA and PBAC.

spectra acquired at the end of each phase (after reaching steady state cycling conditions), i.e., immediately before the transition to rich and the transition to lean. For both PBA and PBAC, the spectra in each phase are dominated by three main bands at 1335, 1418 and 1550 cm^{-1} . The first two bands are ascribed to Ba nitrates, while the third corresponds to Ba carbonate. Given the intensity of the Ba nitrate bands, it is clear that a significant fraction of the nitrate species remained on the surface during cycling and was not removed during the rich phase purge. The reduced intensity of the nitrate bands with increasing temperature can be ascribed to the reduced thermal stability of the nitrate and improved regeneration efficiency. Two additional small bands appeared at 2163 and 2070 cm^{-1} during the rich phase, assigned to Ba–NCO and Pt–CO, respectively. For PBA, the Pt–CO band was observed at 200 and 300 °C, while the Ba–NCO band reached its maximum intensity at 300 °C, and then disappeared at 400 °C. In the case of PBAC (Fig. 8b), the spectra are very similar to those of PBA, mainly

consisting of Ba nitrate bands. Since the carbonate bands overlapped with the cerium nitrate bands at $\sim 1550 \text{ cm}^{-1}$, it is not possible to ascertain how much cerium nitrate was formed during the lean phase. However, different from PBA, no Ba–NCO and Pt–CO bands were observed during the rich phase purge for PBAC, which is again indicative of increased CO consumption over PBAC due to the WGS reaction and ceria reduction.

The spectral changes that occur upon switching between the lean and rich phases are most readily apparent from difference spectra. Fig. 9 shows the difference spectra obtained by subtracting the rich phase spectra from the corresponding lean phase spectra for PBA and PBAC. In both cases, the resulting spectra contain two positive bands at ~ 1320 and 1420 cm^{-1} (Ba nitrate) and one negative band at 1550 cm^{-1} (Ba carbonate), implying that during the rich phase nitrate was removed, with the vacant storage sites on the Ba phase being converted to BaCO_3 . Given that the difference in the intensity of the Ba nitrate bands between the lean

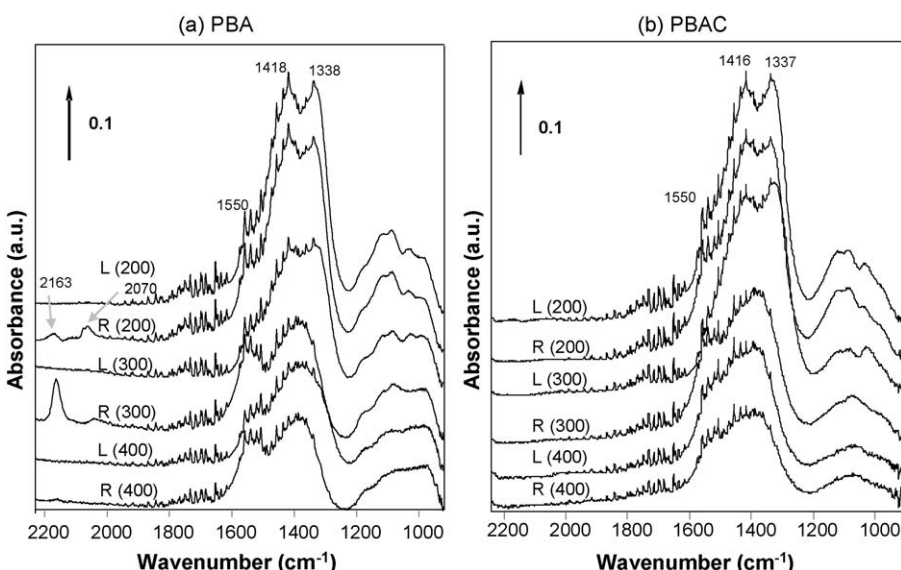


Fig. 8. DRIFT spectra recorded during lean-rich cycling.

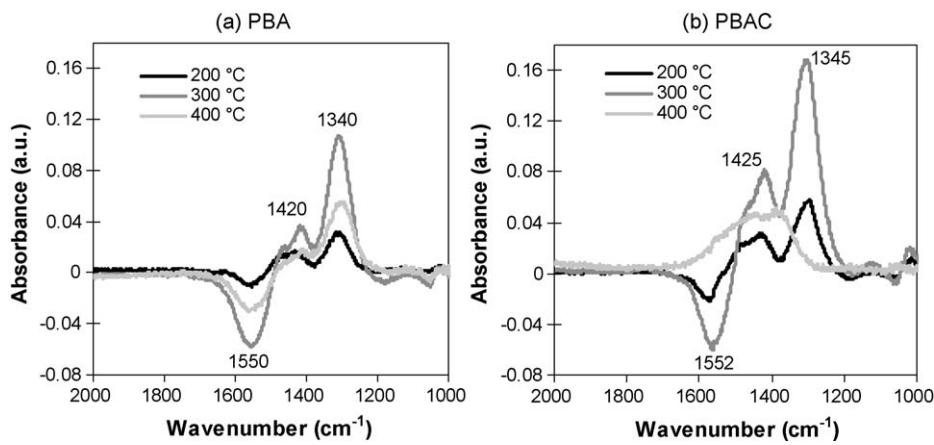


Fig. 9. Difference spectra for PBA and PBAC during lean-rich cycling.

and rich phases is a function of the NO_x conversion during cycling, it is evident that the highest NO_x conversion was obtained at 300 °C for both catalysts, consistent with our previous microreactor studies [16]. Furthermore, relative to the difference spectra at 200 and 400 °C, at 300 °C the difference in the intensity of the lean phase and rich phase nitrate bands was greater for catalyst PBAC than for PBA, implying that NO_x conversion was higher over PBAC than over PBA. This observation is also consistent with our microreactor experiments [16].

4. Conclusions

The main conclusions from this study can be summarized as follows:

- For both NO/O_2 and NO_2/O_2 storage on PBA, nitrite formation was observed at 200 °C during the initial stages of adsorption. In both cases, increasing the adsorption temperature appeared to facilitate the oxidation of nitrite to nitrate. Catalyst PBAC afforded similar DRIFT spectra under these conditions, although the presence of cerium nitrates was observed at 200 and 300 °C, consistent with NO_x storage on the ceria phase.
- During NO_x reduction in H_2 , nitrate was removed at slightly lower temperatures for PBAC as compared to PBA. This is consistent with previously reported TPR experiments and may be a consequence of reduced bulk Ba nitrate formation on PBAC due to competitive capture of NO_x by the ceria phase.
- DRIFT spectra acquired during NO_x reduction in CO -only and CO/H_2 showed that Ba nitrate species remained on the surface of PBA and PBAC at 450 °C, whereas the use of H_2 -only resulted in complete removal of stored NO_x . The observation of Ba carbonates when CO was present suggests that the inferior reduction efficiency of CO may arise from the formation of a crust of BaCO_3 on the Ba phase, which inhibits further NO_x reduction.
- During reduction in $\text{CO}/\text{H}_2\text{O}$, DRIFTS indicated the presence of isocyanate on PBA, whereas isocyanate was not observed for the ceria-containing catalyst. Furthermore, the Pt–CO band disappeared at a lower temperature for PBAC (~250 °C) than for PBA (~300 °C). These findings are indicative of increased CO reactivity on the ceria-containing catalyst, via participation in the water–gas shift reaction, NO_x reduction and reduction of the ceria phase.
- During lean-rich cycling under simulated exhaust gas conditions with CO/H_2 as the rich phase reductants, a significant concentration of nitrates remained on the surface of both PBA and PBAC at the end of the rich phase. This implies that a large fraction of nitrate is not decomposed during cycling and thus cannot participate in NO_x abatement through storage and regeneration.

Acknowledgements

This publication was prepared with the support of the US Department of Energy, under Award no. DE-FC26-05NT42631. However, any opinions, findings, conclusions, or recommendations expressed herein are those of the authors and do not necessarily reflect the views of the DOE.

References

- W.S. Epling, L.E. Campbell, A. Yezerski, N.W. Currier, J.E. Parks II, *Cat. Rev. Sci. Eng.* 46 (2) (2004) 163.
- S. Matsumoto, *Toyota Tec. Rev.* 44 (1994) 10.
- J. Kaspar, P. Fornasiero, M. Graziani, *Catal. Today* 50 (1999) 285.
- M. Haneda, T. Morita, Y. Nagao, Y. Kintaichi, H. Hamada, *Phys. Chem. Chem. Phys.* 3 (2001) 4696.
- Y. Ji, T.J. Toops, U. Graham, G. Jacobs, M. Crocker, *Catal. Lett.* 110 (2006) 29.
- S. Philipp, A. Drochner, J. Kunert, H. Vogel, J. Theis, E.S. Lox, *Top. Catal.* 30–31 (2004) 235.
- M.O. Symalla, A. Drochner, H. Vogel, S. Philipp, U. Göbel, W. Müller, *Top. Catal.* 42–43 (2007) 199.
- E. Rohart, V. Bellière-Baca, K. Yokota, V. Harlé, C. Pitois, *Top. Catal.* 42–43 (2007) 71.
- G. Jacobs, L. Williams, U. Graham, D.E. Sparks, B.H. Davis, *Appl. Catal. A* 252 (2003) 107.
- J. Theis, J. Ura, C. Goralski Jr., H. Jen, E. Thanasiu, Y. Graves, A. Takami, H. Yamada, S. Miyoshi, *SAE Technical Paper* 2003-01-1160 (2003).
- M. Piacentini, M. Maciejewski, A. Baiker, *Appl. Catal. B* 72 (2007) 105.
- M. Casapu, J.-D. Grunwaldt, M. Maciejewski, M. Wittrock, U. Göbel, A. Baiker, *Appl. Catal. B* 63 (2006) 232.
- M. Eberhardt, R. Riedel, U. Göbel, J. Theis, E.S. Lox, *Top. Catal.* 30–31 (2004) 135.
- E.C. Corbos, X. Courtois, N. Bion, P. Marecot, D. Duprez, *Appl. Catal. B* 80 (2008) 62.
- E.C. Corbos, S. Elbouazzaoui, X. Courtois, N. Bion, P. Marecot, D. Duprez, *Top. Catal.* 42–43 (2007) 9.
- Y. Ji, T.J. Toops, M. Crocker, *Catal. Lett.* 119 (2007) 257.
- Y. Ji, J.-S. Choi, T.J. Toops, M. Crocker, M. Naseri, *Catal. Today* 136 (2008) 146.
- F. Frola, F. Prinetto, G. Ghiootti, L. Castoldi, I. Nova, L. Lietti, P. Forzatti, *Catal. Today* 126 (2007) 81.
- I. Malpartida, M.O. Guerrero-Pérez, M.C. Herrera, M.A. Larrubia, L.J. Alemany, *Catal. Today* 126 (2007) 162.
- U. Elizundia, R. López-Fonseca, I. Landa, M.A. Gutiérrez-Ortiz, J.R. González-Velasco, *Top. Catal.* 42–43 (2007) 37.
- Y. Su, K.S. Kabin, M.P. Harold, M.D. Amiridis, *Appl. Catal. B* 71 (2007) 207.
- T. Szailer, J.H. Kwak, D.H. Kim, J.C. Hanson, C.H.F. Peden, J. Szanyi, *J. Catal.* 239 (2006) 51.
- H. Abdulhamid, J. Dawody, E. Fridell, M. Skoglundh, *J. Catal.* 244 (2006) 169.
- I. Nova, L. Castoldi, L. Lietti, E. Tronconi, P. Forzatti, F. Prinetto, G. Ghiootti, *J. Catal.* 222 (2004) 377.
- C. Pazé, G. Gubitosa, S. Orso Giaccone, G. Spoto, F.X. Llabrés i Xamena, A. Zecchina, *Top. Catal.* 30/31 (2004) 169.
- Y. Su, M.D. Amiridis, *Catal. Today* 96 (2004) 31.
- F. Prinetto, G. Ghiootti, I. Nova, L. Castoldi, L. Lietti, E. Tronconi, P. Forzatti, *Phys. Chem. Chem. Phys.* 5 (2003) 4428.
- Ch. Sedlmair, K. Seshan, A. Jentys, J.A. Lercher, *J. Catal.* 214 (2003) 208.
- T. Lesage, C. Verrier, P. Bazine, J. Saussey, M. Daturi, *Phys. Chem. Chem. Phys.* 5 (2003) 4435.

- [30] F. Prinetto, G. Ghiotti, I. Nova, L. Lietti, E. Tronconi, P. Forzatti, *J. Phys. Chem. B* 105 (2001) 12732.
- [31] T. Lesage, J. Saussey, S. Malo, M. Hervieu, C. Hedouin, G. Blanchard, M. Daturi, *Appl. Catal. B* 72 (2007) 166.
- [32] T.J. Toops, D.B. Smith, W.P. Partridge, *Appl. Catal. B* 58 (2005) 245.
- [33] T.J. Toops, D.B. Smith, W.P. Partridge, *Catal. Today* 114 (2006) 112.
- [34] H. Abdulhamid, E. Fridell, J. Dawody, M. Skoglundh, *J. Catal.* 241 (2006) 200.
- [35] Z. Liu, J.A. Anderson, *J. Catal.* 228 (2004) 243.
- [36] P.T. Fanson, M.R. Horton, W.N. Delgass, J. Lauterbach, *Appl. Catal. B* 46 (2003) 393.
- [37] G.L. Powell, M. Milosevic, J. Lucania, N.J. Harrick, *Appl. Spectrosc.* 46 (1992) 111.
- [38] Z. Liu, J.A. Anderson, *J. Catal.* 224 (2004) 18.
- [39] P. Jozsa, E. Jobson, M. Larsson, *Top. Catal.* 30–31 (2004) 177.
- [40] U. Elizundia, R. Lopez-Fonseca, I. Landa, M.A. Gutierrez-Ortiz, J.R. Gonzalez-Velasco, *Top. Catal.* 42–43 (2007) 37.
- [41] Y. Chi, S.S.C. Chuang, *J. Phys. Chem. B* 104 (2000) 4673.
- [42] A. Desikusumastuti, T. Staudt, H. Gronbeck, J. Libuda, *J. Catal.* 255 (2008) 127.
- [43] E. Roedel, A. Urakawa, S. Kureti, A. Baiker, *Phys. Chem. Chem. Phys.* 10 (2008) 6190.
- [44] N.W. Cant, M.J. Patterson, *Catal. Today* 73 (2002) 271.
- [45] T. Szailer, J.H. Kwak, D.H. Kim, J. Szanyi, C. Wang, C.H.F. Peden, *Catal. Today* 114 (2006) 86.
- [46] D. James, E. Fourre, M. Ishii, M. Bowker, *Appl. Catal. B* 45 (2003) 147.
- [47] J. Theis, H.-W. Jen, R. McCabe, M. Sharma, V. Balakotaiah, M.P. Harold, *SAE Technical Paper Series* 2006-01-1067 (2006).
- [48] I. Nova, L. Castoldi, L. Lietti, E. Tronconi, P. Forzatti, *SAE Technical Paper Series* 2006-01-1368 (2006).
- [49] E. Shustorovich, A.T. Bell, *Surf. Sci.* 289 (1993) 127.
- [50] R. Burch, T.C. Watling, *Catal. Lett.* 37 (1996) 51.
- [51] N. Macleod, R.M. Lambert, *Appl. Catal. B* 46 (2003) 483.
- [52] B. Westerberg, E. Fridell, J. Mol. Catal. 165 (2001) 249.
- [53] C.M.L. Scholz, B.H.W. Maes, M.H.J.M. de Croon, J.C. Schouten, *Appl. Catal. A* 332 (2007) 1.